cigre Turkey

TEPES
TURKISH JOURNAL OF
ELECTRICAL POWER
AND ENERGY SYSTEMS

TEPES, Vol. 2, Issue. 1, 85-93, 2022 DOI: 10.5152/tepes.2022.22009

RESEARCH ARTICLE

Analysis of Solid Insulating Materials Breakdown Voltages Under Different Voltage Types

Firat Akın[1], Oktay Arıkan[1], Cihat Çağdaş Uydur[2]

[1]Department of Electrical Engineering, Yıldız Technical University, İstanbul, Turkey
[2]Technical Science Vocational School, Trakya University, Edirne, Turkey

Cite this article as: F. Akin, O. Arikan and C. Cagdas Uydur, Analysis of solid insulating materials breakdown voltages under different voltage types. *Turk J Electr Power Energy Syst,* 2022; 2(1): 85-93.

ABSTRACT

The effectiveness of the insulation systems has great importance for the continuity of the power equipment. Due to operating conditions, solid insulating materials are subjected to different types of stresses. In this context, one of the factors affecting the breakdown performance is the type of the applied voltage. Since the breakdown strength of the materials determines their lifespan, the effect of the different voltage types must be considered for proper insulation design. For this reason, it is vital to investigate the breakdown performance of insulation materials under different voltage types. In this study, breakdown voltages of press-paper, polyethylene terephthalate and styrene–butadiene rubber/natural rubber under AC, positive DC(+), and negative DC(−) voltages were investigated. For the analysis of the breakdown points, the electric field analysis of the materials for the cylinder–cylinder electrode configuration was performed with COMSOL Multiphysics® software. As a result, it was determined that the electric field distortion increased in the triple junction regions and the potential breakdown points obtained by the simulation matched with seen in the experiments.

Index Terms—Breakdown voltage, electric field analysis, COMSOL multiphysics, solid insulating materials, permittivity

I. INTRODUCTION

Solid insulating materials are the primary elements of the insulation systems of most power equipment. In this context, the dielectric performance of solid insulating materials under different operating conditions should be examined in detail to ensure the continuity of power systems. The breakdown mechanism of solid materials is irreversible, unlike other materials. That is, once degradation occurs, they cannot revert to their former dielectric properties. Therefore, in order to use solid dielectrics efficiently, the mechanisms that can cause degradation should be well known [1,2].

Solid insulation materials are preferred for the insulation of both DC and AC equipment. In addition, the dielectric performances vary considerably under these voltages. Therefore, when examining the breakdown strength of solid insulation materials, different voltage types should be considered, and the conditions covering all the negativities that may occur during the operation of power systems should be investigated.

In a study, breakdown experiments were carried out on Teflon, quartz–silica, and glass–ceramic materials using AC, DC, and impulse voltages. It has been revealed that AC breakdown voltages have the lowest values in all materials and the highest breakdown voltage was reached when AC + DC combined voltage was applied. In addition, it was seen that the AC breakdown voltages of the materials were not affected by the DC pre-stress, while the DC breakdown voltages decreased in the case that DC pre-stress with opposite polarity was applied to the specimens [3]. In the study of Rajan et al., the breakdown voltage of oil-impregnated paper under AC and DC voltages was investigated. They determined that the breakdown performance was better in the experiments performed with DC voltage. Lastly, it was stated that the results are unpredictable when AC and DC voltages are combined [4]. In the studies realized by Grzybowski et al., breakdown voltages of Cross-linked Polyethylene (XLPE) and polyethylene terephthalate (PET) materials were investigated under dry and wet conditions. In this study, it was shown that DC breakdown voltage decreased significantly compared to the AC breakdown

Corresponding author: Cihat Çağdaş Uydur, ccagdasuydur@trakya.edu.tr

Received: February 7, 2022
Accepted: March 27, 2022

Content of this journal is licensed under a Creative Commons Attribution-NonCommercial 4.0 International License.

voltage under wet conditions compared to dry conditions [5-7]. In another study, the change in the breakdown performance of polymeric insulation materials as a result of thermal aging was investigated using AC, DC, and pulsed voltages [8]. Nagao et al. measured the breakdown strength of various insulating material variations formed with kraft paper and polypropylene laminations under AC, DC, and impulse voltages in liquid nitrogen. It has been found that the breakdown performance was affected by the lamination structures of the materials due to the changes in the electric field and charge behaviors [9]. In a study, the breakdown performance of the solid dielectric barriers inserted between the electrodes under non-uniform electric fields by experimental and simulation studies was investigated by Phloymuk. According to the measurement results, it has been seen that the AC breakdown voltage was lower than the DC breakdown voltage. In addition, it was emphasized that the critical pressure was 1.5 bar in the experiments carried out at different pressures. Below the critical pressure, the positive DC breakdown voltage was higher than the negative DC breakdown voltage, and the opposite case was seen at pressures above the critical value [10]. Illias et al. experimentally investigated partial discharges originating from spherical voids in solid insulating materials [11,12]. A similar research was also carried out by simulation studies and the correlation between simulation results and experiments was clearly seen. As a result, the partial discharges have been defined as a function depending on the temperature and the voltage type [13,14]. Yamada studied the breakdown mechanisms of dielectric elastomers under different applied waveforms (DC, AC, and pulse). It has been found that the breakdown strengths have the order of impulse > DC > AC. Also, the breakdown strengths under these waveforms decreased as the temperature increases. He attributed the lowest breakdown strength under AC voltage to the heating that occurs as a result of dielectric losses under AC voltage. Moreover, the study revealed that the number of laminations leads to an increase in breakdown strength [15]. In another study, DC and AC breakdown characteristics of polypropylene laminated paper as well as various Nomex and Kapton insulating materials were investigated in air and liquid nitrogen. The difference between the Weibull scale parameters of DC and AC breakdown voltages of materials was found as 1.12–1.72 times in air and 1.52–2.14 times in liquid nitrogen [16,17]. In the studies performed by Barouel et al., the breakdown strength of vegetable and mineral oils under AC and DC voltages was studied, and the analysis of dielectric performance of different oil mixtures was carried out for the specified voltages [18,19]. In one study, Huang explores the possibility of improving both the mechanical and degradation properties of insulating printing paper by adding an organic nanoadditive, taking into account four different concentrations of nanofibrillated cellulose (NFC) such as 0.5% by weight, 2.5% by weight, 5% by weight, and 10% by weight. The prepared samples were characterized by scanning electron microscopy, Fourier transform infrared spectroscopy, and X-ray diffraction. It has been found that the addition of 10 wt% NFC provides the best performance in terms of breakdown voltage, and the presspaper containing 10 wt% NFC had 19% and 21% higher AC and DC breakdown voltages than the reference material [20]. Furthermore, studies on the definition and classification of partial discharges were continued by examining them under different voltage types such as impulse voltages and damped voltages [21,22]. In this context, there are also simulative studies to examine the breakdown strength of insulating materials. In these studies, COMSOL Multiphysics® software was preferred [23,24].

Main Points

- Experimental studies have been carried out in the high-voltage laboratory.
- Breakdown voltages of different solid insulating materials were measured with DC+, DC−, and AC voltage types.
- Analysis of electric field distribution studies had been carried out using COMSOL Multiphysics® software.
- Breakdown points that occurred in test specimens had been detected.

In this research, an experimental study was carried out to analyze breakdown performances of solid insulating materials under different types of voltages. Test specimens of 60 × 60 mm^2 dimensions were created from solid insulation materials that were widely used in power systems, PET, presspaper, and a mixture of styrene–butadiene rubber/natural rubber (SBR/NR). As the test voltage, AC, positive DC(+), and negative DC(−) voltages were preferred. Experimental studies were made in Yıldız Technical University High Voltage Laboratory. Finally, an electric field analysis was performed in COMSOL Multiphysics® to explain and analyze the breakdown points seen in the experiment. From the results of the electric field analysis, the location where the breakdown occurred was evaluated.

II. TEST MATERIALS

To examine the effect of voltage type on different classes of insulating materials, PET from thermoplastic polyesters, SBR/NR blend from thermoset polymers, and presspaper, which is an organic insulating material, were used in this study.

Presspaper used in the experiments is fundamental element of oil-type transformer insulation. It is obtained by calendaring kraft paper, and it consists of sulphate–cellulose. Because of their high operating temperatures, resilience to various chemicals, and good dielectric qualities, PET films are commonly preferred in stator slots and interlayer insulations of high-voltage machines. As is known, it is common application to optimize the properties of rubber types by mixing them and use them in the form of blends. Another insulator used in this study is SBR/NR, which is a blend of rubbers. It is commonly used in cable insulation and dielectric matting. The samples of the materials are shown in Fig. 1.

The surface dimensions of the samples were determined as 60 mm × 60 mm with preliminary studies to prevent surface discharges. The specifications of the samples are given in Table 1.

III. EXPERIMENTAL STUDY

In this chapter, the laboratory conditions, the electrode system used in the experimental applications, and the experimental setup were introduced. In addition, the results of the breakdown voltage tests obtained from the experimental measurements are shared in a comparative manner depending on the material and voltage types.

Fig. 1. Test specimens (PET, presspaper, and SBR/NR).

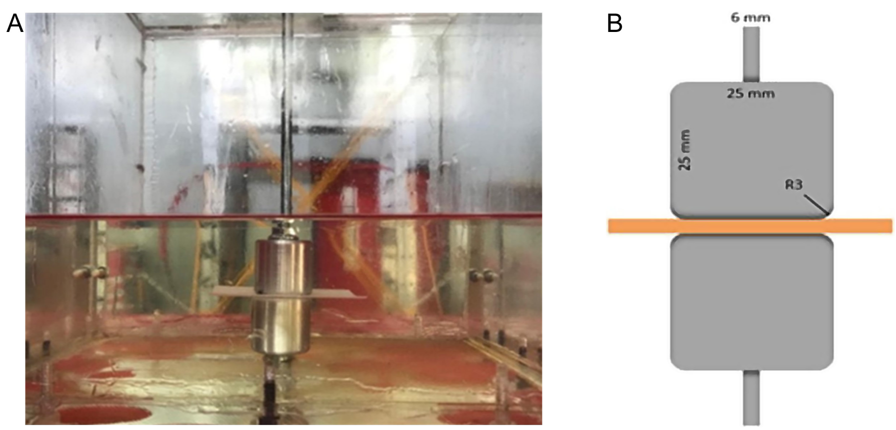

Fig. 2 (a) Electrode configuration and (b) dimensions.

A. Experimental Setup

Ambient conditions in laboratory during the experiments were 28 $\pm$ 2°C temperature, 41 $\pm$ 2% relative humidity, and 756.8 $\pm$ 5 mmHg pressure. Cylinder–cylinder aluminum electrode system was used in accordance with IEC60243:1 [25]. Details are shown in Fig. 2.

Fig. 2a shows the cylinder–cylinder electrode system in the laboratory, and Fig. 2b shows the dimensions of the electrode system in accordance with the IEC 60243:1 standard and its positioning on the insulating material.

For preventing surface discharges, electrodes and specimens were immersed in Nytro Lyra X mineral oil (BDV > 60 kV, $\varepsilon_r = 2.2$). The tests were repeated five times for each material, and 3 minutes was given between trials. The surfaces of all samples were cleaned with ethanol before the measurements. The scheme of the experimental setup is shown in Fig. 3.

To generate the test voltages, 100 kV, 5 kVA single phase, and 50 Hz frequency test transformer was used. DC voltages are obtained with a high-voltage diode. The test voltage was increased until breakdown occurs, and the breakdown voltages were measured with a resistive voltage divider (1000:1 ratio) for DC measurements and capacitive voltage divider (1000:1 ratio) for AC measurements.

B. EXPERIMENTAL RESULTS

In this section, the measurement results according to the specified voltage types are shared for each insulation material. In order to evaluate the results obtained by repeated tests, box-plot notation, which is a statistical presentation form, was preferred. Breakdown voltages are demonstrated as the average value for DC voltages and the peak values for AC voltages.

Fig. 4 demonstrates the breakdown voltages of PET. In the tests performed under AC voltage, the minimum and maximum breakdown voltages of five samples were 26.96 kV and 30.03 kV. In this case, the average breakdown voltage was calculated as 28.37 kV. Under positive DC, the breakdown voltages were between 40.3 kV and 54.2 kV with an average of 44.74 kV. Finally, PET failed at the voltages between 43.81 kV and 50.5 kV under negative DC, while the average value was 47.72 kV. From the results, effectiveness of AC voltage was found significantly higher than DC voltage types for PET.

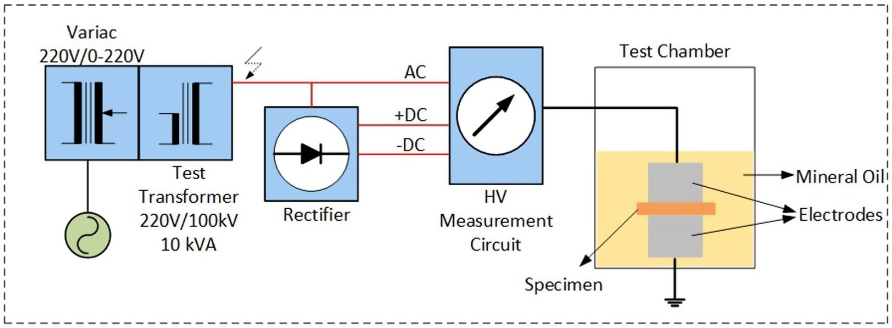

Fig. 3. Scheme of experimental setup.

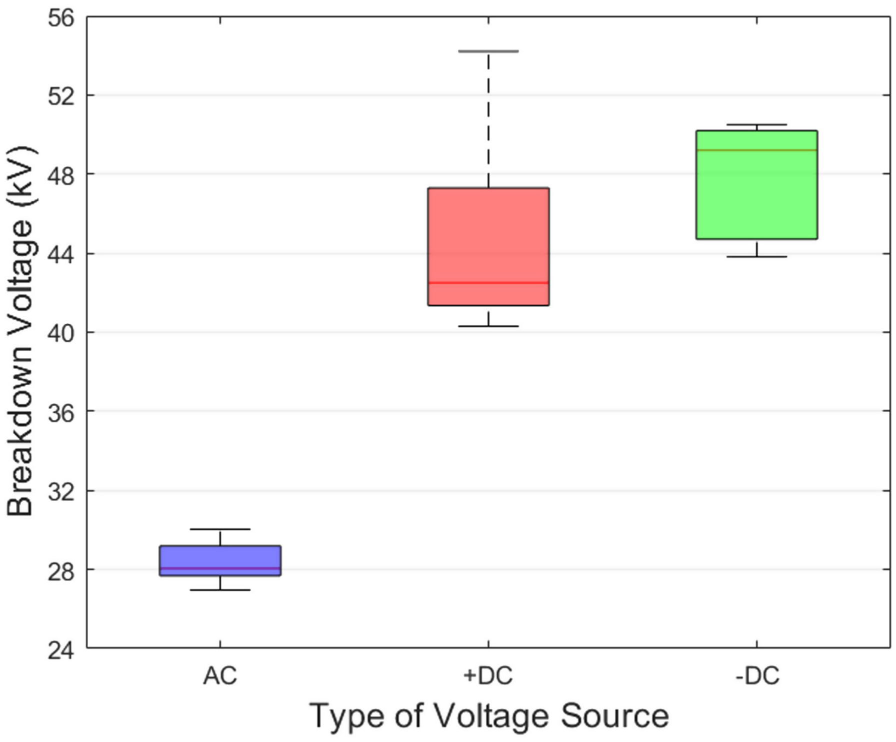

Fig. 4. Box plot of breakdown voltages—PET.

When the breakdown voltage values for presspaper shown in Fig. 5 are examined, it was seen that AC voltage punctured the material at around 50% lower voltage values, according to DC voltage types. It has been found that positive and negative DC voltages provide very close results. The breakdown voltages measured with different voltage types had the values in the ranges of 6.08–8.38 kV, 8.33–12.83 kV, 9–13.56 kV for AC, positive DC, and negative DC, respectively. The average breakdown voltage for AC was 7.26 kV, while these values were 10.85 kV and 10.95 kV for positive and negative DC voltages.

In the case of SBR/NR, it was determined that the effectiveness of AC voltage was greater than DC as with the other materials. Box graph of breakdown voltages for SBR/NR is shared in Fig. 6. As can be seen, the breakdown voltages obtained with AC voltage varied between 47.37 kV and 64.86 kV. The average of these values was 57.75 kV. Also, the breakdown voltages of the material under positive DC voltage varied between 56.87 kV and 62.81 kV with an average of 60.83 kV. When negative DC voltage was applied to the material, the minimum and maximum breakdown voltages of five samples were 58.94 kV and 66 kV. The average of these values was 62.32 kV.

IV. INVESTIGATION ON BREAKDOWN POINTS OF THE MATERIALS

In this section, electric field analyses of the materials are performed with electrostatic interface under the AC/DC module of COSMOL Multiphysics® software to investigate the potential breakdown points.

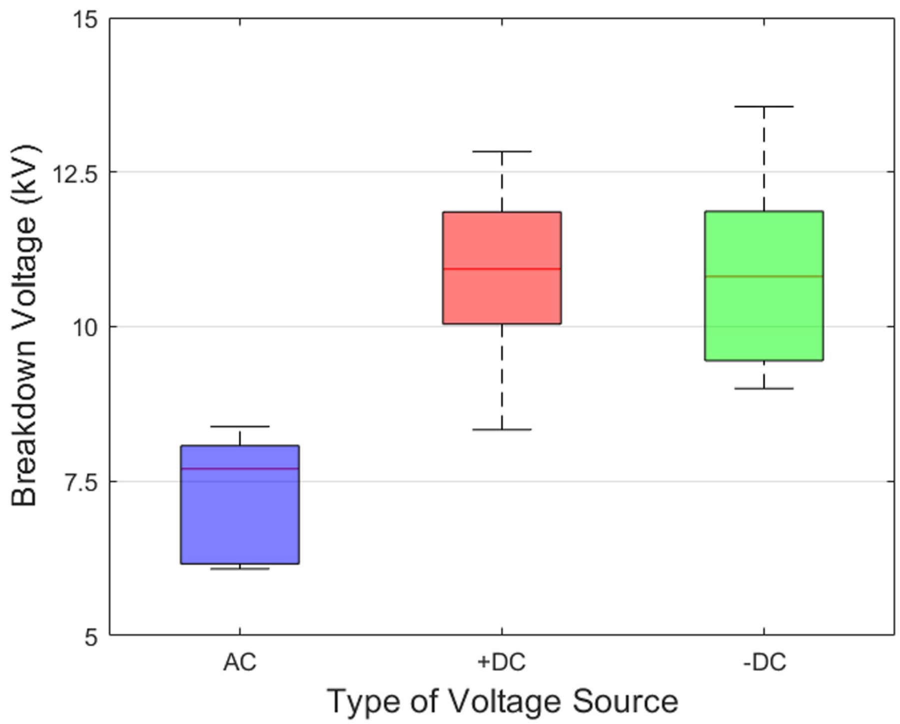

Fig. 5. Box plot of breakdown voltages—presspaper.

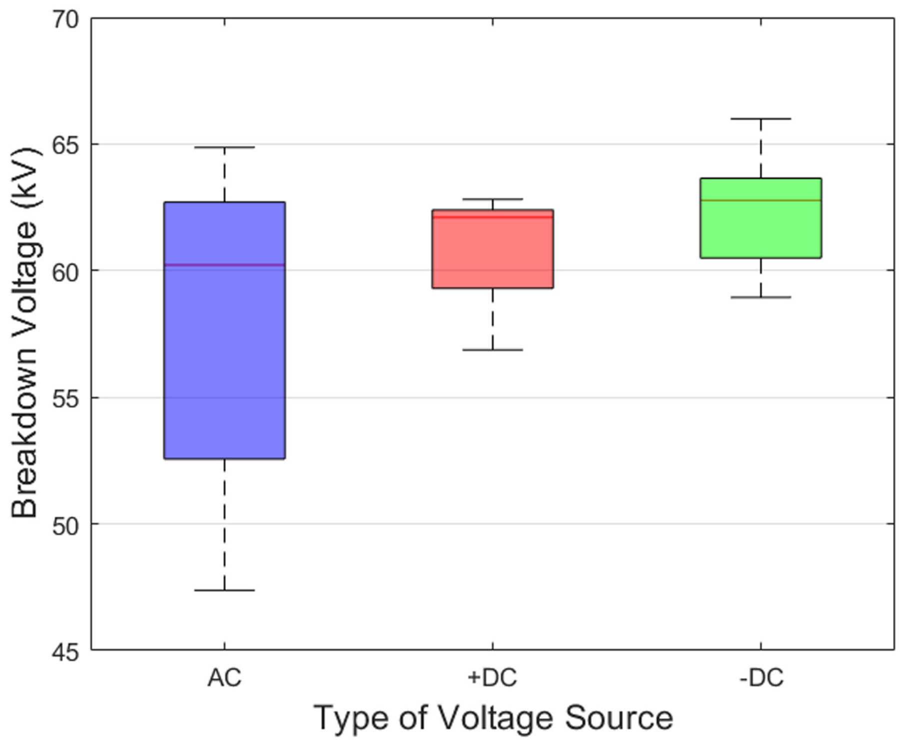

Fig. 6. Box plot of breakdown voltages—SBR/NR.

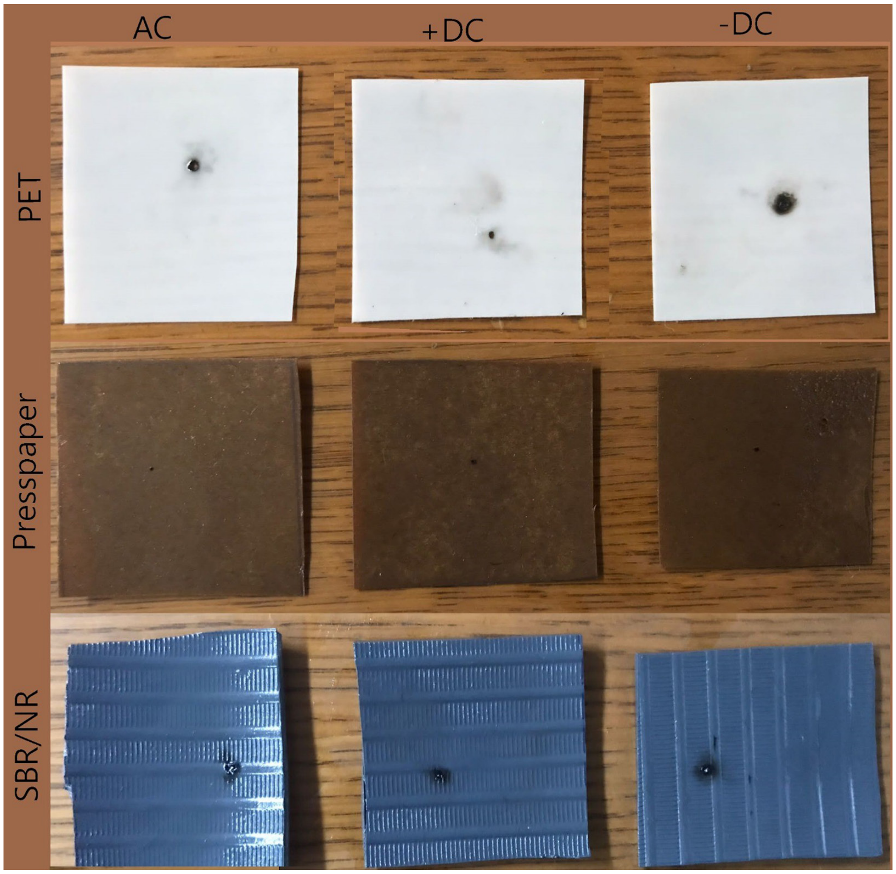

Fig. 7. Breakdown samples of the materials.

As can be seen in Fig. 7, the breakdowns occurred at the electrode boundary areas for all voltage types. For examining this case, the average AC breakdown voltages of the insulating materials are applied during the simulation study, and the electric field densities along their upper surfaces are calculated. The governing equations applied by COMSOL Multiphysics® to solve the defined electrostatic problem are as follows [26]:

$$\nabla \times E = 0 \tag{1}$$

The above formula shows that the electric field is irrotational.

$$\nabla . D = \rho \tag{2}$$

$$-\nabla V = E \tag{3}$$

$$D = \varepsilon_r \varepsilon_0 E \tag{4}$$

By substituting the electric field and displacement expressions specified in (3) and (4) into (2), (5) is obtained, which shows the relationship between the electrostatic potential and the space charge density.

$$-\nabla .(\varepsilon_r \varepsilon_0 \nabla V) = \rho \tag{5}$$

where E is the electric field density, D is the electric displacement, ρ is space charge density, ε_0 is the permittivity of free space, and ε_r is the relative permittivity of insulating material.

A simulation model for SBR/NR and the triple area region where the electric field is concentrated are shown in Fig. 8.

As a result of the simulation, it was found that the breakdown occurred at a distance of 20 $\pm$ 2 mm from the one edge of the insulating materials, and the breakdown strengths of presspaper, PET, and SBR/NR were 23.59 kV/mm, 114.98 kV/mm, and 41.04 kV/mm, respectively.

The change in the electric field magnitude along the upper surface of the insulating materials is shown in Fig. 9. The electric field density reaches its highest value at the boundary points where the corners of the electrodes begin to round. When the failed samples are examined, the breakdown points and the possible breakdown points obtained in the simulation study match with each other.

V. DISCUSSION

Average breakdown voltages of the materials according to voltage types are given in Fig. 10. The lowest breakdown voltages for all insulation materials were obtained in the experiments with AC voltage. For PET, the average breakdown voltages under positive DC and negative DC voltages were 57.7% and 68.2% higher than AC, respectively. The average DC breakdown voltages of presspaper were 49.44% and 51% higher than AC breakdown voltages for positive and negative polarities, respectively. The change in the DC breakdown voltage

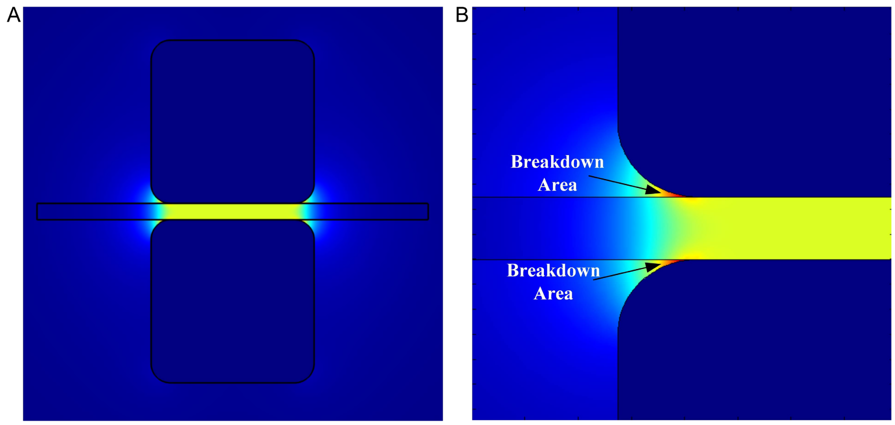

Fig. 8. (a) Electrode system and (b) breakdown areas in simulation model.

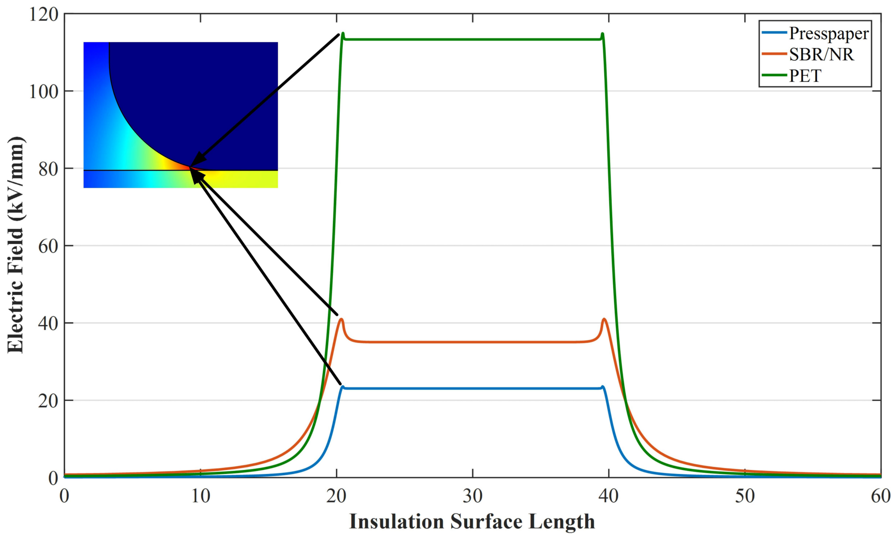

Fig. 9. Variation of electric field density along the electrode–material contact surface.

due to polarity was less for presspaper, unlike other materials. The average breakdown voltage of SBR/NR was 57.75 kV under AC voltage. It increased by 5.33% to 60.83 kV under positive DC voltage and increased by 7.91% to 62.32 kV under negative DC voltage. The breakdown performance of SBR/NR was less affected by the applied voltage type than the other materials. The fact that AC breakdown voltages have lower values in all materials can be explained by two phenomena. These are the dielectric losses that occur in the insulating material exposed to AC voltage and the difference of space charge behavior at AC and DC voltages. A significant heating occurs in the material due to dielectric losses, and it affects the dielectric performance of the insulating material by causing them to fail at lower voltage levels [6].

The structure and accumulation points of space charges become different depending on applied voltage type. When AC voltage is applied, space charges accumulate around the electrodes and have a heterogeneous structure. In the case of DC test voltage, there is a homogeneous structure, and the accumulation point of the charges is the middle of the insulation bulk. Hetero-charges accumulation in the vicinity of the electrodes causes the distortion of the electric field dramatically in these regions. In addition, when charges accumulate in the vicinity of the electrode, smaller transport distance for charges is required compared to DC voltages, where the charge accumulation is in the middle of the insulation bulk. Due to all these facts, breakdown occurs at lower voltage levels, as more severe electric fields will occur under AC voltages [27-29].

While examining the weakest points of the materials in COSMOL Multiphysics®, it is determined that the mismatch between the permittivities of the test specimens and the surrounding material (in this case mineral oil) at the triple contact area causes an increase in the electric field magnitude. Electric field density along the upper surface reaches its maximum value at that area. In addition, as the relative permittivity of the insulating material increases, the difference between the electric field densities at triple contact point and the bottom of the high-voltage electrode increases. While the electric field intensity at the triple contact point of SBR/NR was 17.15%

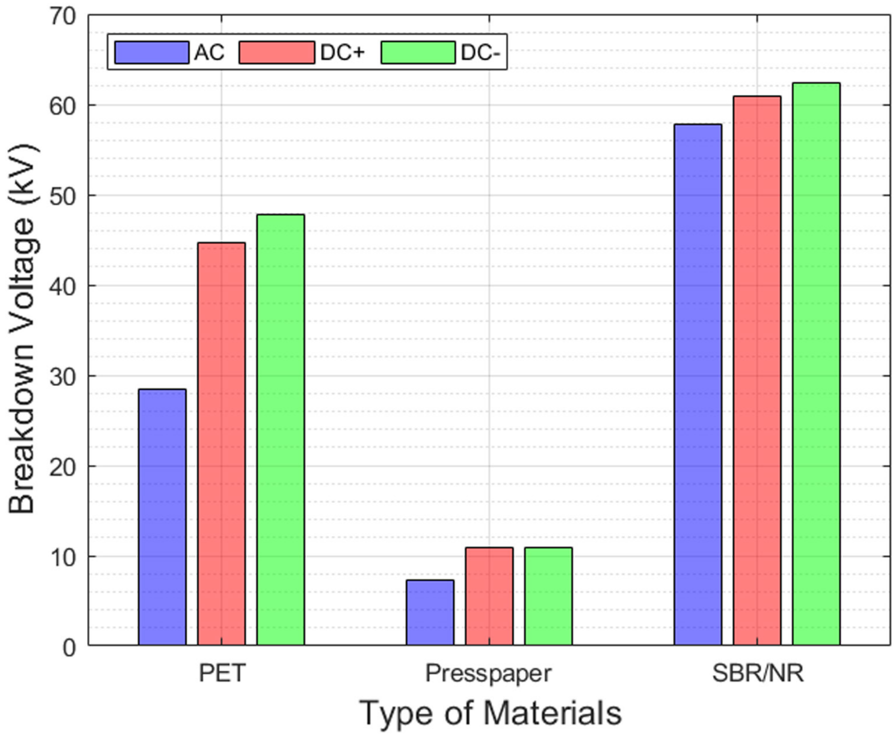

Fig. 10. Average breakdown voltages of materials.

TABLE I
SPECIFICATIONS OF THE SAMPLES

Materials	Thickness	Surface Dimensions (mm × mm)	Relative Permittivity	Tan δ	Max. Operating Temperature (°C)	Density (g/cm³)
PET	0.3	60 × 60	3.2	2×10^{-3}	110	1.39
SBR/NR	2.5	60 × 60	4.5	4×10^{-2}	70	1.45
Presspaper	0.4	60 × 60	3.5	6×10^{-3}	90	1.0-1.2

PET, polyethylene terephthalate; SBR/NR, styrene–butadiene rubber/natural rubber.

higher than the electric field density along the lower surface of the electrode, this difference was 2.3% for presspaper and 1.4% for PET.

VI. CONCLUSIONS

The main subject of this research was the breakdown performances of PET, presspaper, and SBR/NR under AC, positive DC, and negative DC voltages. Also, an Finite Element Method (FEM)-based simulation study was performed in COSMOL Multiphysics for the analysis of the breakdown points obtained in experiments.

During the experimental study, it was found that the breakdown voltages of all materials were in the order of AC < +DC < −DC. In addition, the increase of the average breakdown voltages in the case of negative DC voltage was 50% and 68% for presspaper and PET compared to AC voltage, while the difference in the breakdown voltage of SBR/NR was around 8% for the same comparison. The specified amounts of increases vary according to their physical and chemical structures. The change in breakdown performance between AC and DC voltages was caused by differences in space charge behavior and heating due to dielectric loss. Insulating materials used in power systems can be stressed by different types of voltages. Therefore, understanding the effects of different voltage types on the dielectric performance of insulating materials is vital for power equipment continuity.

In the simulation study, it was determined that the electric field distortion increased in the triple junction areas. Therefore, breakdown occurred in these regions of the samples in accordance with the experimental study. In addition, it has been revealed that the electric field strengths at the electrode boundaries increase in direct proportion to the permittivities of the insulating materials.

The type and rate rise of the test voltage, conductor–insulator geometries, age of the insulating material, permittivity mismatch, and ambient conditions are the primary factors affecting the breakdown performance. For this reason, breakdown performances of the insulating materials should be analyzed by performing simulation and experimental studies including the mentioned factors, and the design of the equipment used in power systems should be developed with the help of the information obtained from the analysis results. In this manner, the reliability and sustainability of the equipment can be ensured by minimizing the failures that occur during the operation of the power systems.

Peer-review: Externally peer-reviewed.

Declaration of Interests: The authors have no conflict of interest to declare.

Funding: Scientific Research Project Coordinator of Yıldız TechnicalUniversity supported this research study with the project number FYL-2021-4166.

REFERENCES

1. N. H. Malik, A. A. Al-Arainy, and M. I. Qureshi, *Electrical Insulation in Power Systems*. Boca Raton: CRC Press, 2018.
2. R. Arora, and W. Mosch, *High Voltage and Electrical Insulation Engineering*. IEEE Press: Piscataway, New Jersey 08854, USA, 2011.
3. A. S. Pillai, and R. Hackam, "Effect of DC pre-stress on AC and DC surface flashover of solid insulators in vacuum," *IEEE Trans. Electr. Insul.*, vol. EI–18, no. 3, pp. 292–300, 1983. [CrossRef]
4. J. S. Sajan, K. Dwarakanath and S. N. Moorching, "Comparative evaluation of dielectric strength of paper-oil insulation under ac, dc, combined, composite ac/dc and impulse voltages," *1998 Annual Report Conference on Electrical Insulation and Dielectric Phenomena* (Cat. No.98CH36257), 1998, pp. 236–239 vol. 1. [CrossRef]
5. S. Grzybowski, and J. Fan, "Electrical breakdown characteristics of the XLPE cables under AC, DC, and pulsating voltages," *Proc. IEEE Int. Conf. Prop. Appl. Dielectr. Mater.*, vol. 1, pp. 389–393, 1997.
6. S. Grzybowski, E. A. Feilat, P. Knight, and L. Doriott, "Breakdown voltage behavior of PET thermoplastics at DC and AC voltages," *Conf. Proc. - IEEE SOUTHEASTCON*, vol. 1999, pp. 284–287, 1999.
7. Y. Wang, J. Li, Y. Wang, and S. Grzybowski, "Electrical breakdown properties of oil-paper insulation under AC-DC combined voltages *Proc*," *Proc. 2010 IEEE Int. Power Modul. High Volt. Conf. IPMHVC*, vol. 2010, pp. 115–118, 2010.
8. W. Yin, and D. Schweickart, "Dielectric breakdown of polymeric insulation films under AC, DC and pulsed voltages," *2009 IEEE Electr. Insul. Conf. EIC 2009*, vol. 2009, pp. 292–296, , 2009.
9. M. Nagao *et al.*, "Dielectric breakdown mechanism of polypropylene laminated paper in liquid nitrogen," *Annu. Rep. - Conf. Electr. Insul. Dielectr, Phenomena, CEIDP*, pp. 419–422, 2011.
10. N. Phloymuk, A. Pruksanubal, and N. Tanthanuch, "DC breakdown voltage of solid dielectric barrier under non-uniform electric field," *Annu. Rep. - Conf. Electr. Insul. Dielectr, Phenomena, CEIDP*, pp. 834–837, 2013.
11. H. A. Illias, G. Chen, and P. L. Lewin, "Partial discharge measurements for spherical cavities within solid dielectric materials under different stress and cavity conditions," *Annu. Rep. - Conf. Electr. Insul. Dielectr, Phenomena, CEIDP*, vol. 2, pp. 388–391, 2009.
12. H. A. Illias, G. Chen, and P. L. Lewin, "Modelling of partial discharge activity in different spherical cavity sizes and locations within a dielectric insulation material," *Proc. IEEE Int. Conf. Prop. Appl. Dielectr. Mater.*, pp. 485–488, 2009.
13. H. A. Illias, G. Chen, and P. L. Lewin, "Modelling of partial discharge behaviour in a spherical cavity within a solid dielectric material as a function of temperature," *Annu. Rep. - Conf. Electr. Insul. Dielectr, Phenomena, CEIDP*, pp. 1–4, 2010.
14. H. Illias, G. Chen, and P. L. Lewin, "Partial discharge behavior within a spherical cavity in a solid dielectric material as a function of frequency and amplitude of the applied voltage," *IEEE Trans. Dielectr. Electr. Insul.*, vol. 18, no. 2, pp. 432–443, 2011. [CrossRef]
15. M. Yamada, Y. Murakami, T. Kawashima, and M. Nagao, "Electrical breakdown of dielectric elastomer and its lamination effect," *2014 IEEE Conf. Electr. Insul. Dielectr. Phenomena, CEIDP*, vol. 2014, pp. 126–129, 2014.
16. W.-G. Li *et al.*, "Comparison between the DC and AC breakdown characteristics of dielectric sheets in liquid nitrogen," *IEEE Trans. Appl. Supercond.*, vol. 24, no. 6, pp. 1–6, 2014. [CrossRef]
17. M. Ritamaki, I. Rytoluoto, M. Niittymaki, K. Lahti, and M. Karttunen, "Differences in AC and DC large-area breakdown behavior of polymer thin films," *Proc. 2016 IEEE Int. Conf. Dielectr. ICD 2016*, vol. 2, pp. 1011–1014, 2016.
18. A. Beroual, H. B. H. Sitorus, R. Setiabudy, and S. Bismo, "Comparative study of AC and DC breakdown voltages in Jatropha methyl ester oil, mineral oil, and their mixtures," *IEEE Trans. Dielect. Electr. Insul.*, vol. 25, no. 5, pp. 1831–1836, 2018. [CrossRef]
19. A. Beroual, U. Khaled, P. S. M. Noah, and H. Sitorus, "Comparative study of breakdown voltage of mineral, synthetic and natural oils and based mineral oil mixtures under AC and DC voltages," *Energies*, vol. 10, no. 4, pp. 1–17, 2017. [CrossRef]
20. J. Huang, Y. Zhou, L. Dong, Z. Zhou, and X. Zeng, "Enhancing insulating performances of presspaper by introduction of nanofibrillated cellulose," *Energies*, vol. 10, no. 5, p. 681, 2017. [CrossRef]
21. H. Illias, J. Low Tau, A. H. A. Bakar, and H. Mokhlis, "Partial discharge simulation under various applied voltage waveforms," *PECon 2012 - 2012 IEEE Int. Conf. Power Energy*, pp. 967–972, 2012.
22. H. Illias, T. S. Yuan, A. H. A. Bakar, H. Mokhlis, G. Chen, and P. L. Lewin, "Partial discharge patterns in high voltage insulation," *PECon 2012 - 2012 IEEE Int. Conf. Power Energy*, pp. 750–755, 2012.
23. M. S. Kamarudin, N. H. Radzi, A. Ponniran, and R. Abd-Rahman, "Simulation of electric field properties for air breakdown using COMSOL multiphysics," In 4th IET Clean Energy and Technology Conference (CEAT 2016), 2016, pp. 1–5.
24. S. Nedphokaew, S. Pukjaroon, and M. Boonthienthong, "Analysis of electric field values in 24 kV high voltage power cable with Program for Finding Partial Discharge Values," In International Conference on Power, Energy and Innovations (ICPEI), vol. 2019, 2019, pp. 110–113.
25. Electric Strength of Insulating Materials - Test Methods - Part 1: Tests at Power Frequencies, IEC standard 60243-1, 2013.
26. "Comsol multiphysics," *An Introduction to the Theory of Electrostatics*.
27. S. Li, Y. Zhu, D. Min, and G. Chen, "Space charge modulated electrical breakdown," *Sci. Rep.*, vol. 6, pp. 32588, 2016. [CrossRef]
28. B. Huang, M. Hao, J. Hao, J. Fu, Q. Wang, and G. Chen, "Space charge characteristics in oil and oil-impregnated pressboard and electric field distortion after polarity reversal," *IEEE Trans. Dielect. Electr. Insul.*, vol. 23, no. 2, pp. 881–891, 2016. [CrossRef]
29. G. Chen, C. Zhou, S. Li, and L. Zhong, "Space charge and its role in electric breakdown of solid insulation," In IEEE International Power Modulator and High Voltage Conference (IPMHVC), 2016, pp. 120–127.